Polarity engineering in polycrystalline ZnO by inversion boundaries

Jong-Lo Park, Chan Park, Doh-Yeon Kim, Wook Jo, Chul-Jae Park, Sang-Yun Jeon, and Jong-Sook Lee

Citation: Applied Physics Letters **94**, 252108 (2009); doi: 10.1063/1.3159823
View online: http://dx.doi.org/10.1063/1.3159823
View Table of Contents: http://scitation.aip.org/content/aip/journal/apl/94/25?ver=pdfcov
Published by the AIP Publishing

Polarity engineering in polycrystalline ZnO by inversion boundaries

Jong-Lo Park,[1] Chan Park,[1,a)] Doh-Yeon Kim,[1,b)] Wook Jo,[2] Chul-Jae Park,[3] Sang-Yun Jeon,[3] and Jong-Sook Lee[3]
[1]*Department of Materials Science and Engineering, Seoul National University, Seoul 151-744, Republic of Korea*
[2]*Institute of Materials Science, Technische Universität Darmstadt, 64287 Darmstadt, Germany*
[3]*School of Materials Science and Engineering, Chonnam National University, Gwangju 500-757, Republic of Korea*

(Received 29 April 2009; accepted 6 June 2009; published online 25 June 2009)

Two distinctive polarity-engineered microstructures were obtained in polycrystalline ZnO ceramics by inducing two different types of inversion boundaries (IBs) inside individual grains to examine the effect of the different polarities on the varistor performances. The presence of head-to-head IBs induced by the addition of Sb and tail-to-tail IBs by doping Ti was directly confirmed by the characteristic geometry of the chemical etch pits. It was proposed that a consequent polarity on the grain boundary planes, which are affected by the presence of head-to-head IBs is crucial in exhibiting the superior performance of ZnO varistors. © *2009 American Institute of Physics*.
[DOI: 10.1063/1.3159823]

Zinc oxide is an archetypal electroceramics commercialized as surge protectors. A consensus has been made that a Schottky barrier forming at the grain boundaries (GBs) plays a crucial role in the varistor performance, but the exceptionally superior performances of the commercialized varistors have not been clearly understood yet.[1,2] Noting that all commercially produced ZnO varistors contain polarity inversion boundaries (IBs), which bisect individual grains [e.g., see Fig. 2(a)], a series of experiments have been conducted on the role of IBs on varistor performances.[3,4] However, the electrical characterization on the individual IBs revealed that IBs do not exhibit varistor characteristics, and thus little attention has been paid to the role of IBs on the varistor properties afterwards.

Systematic studies on *I-V* characteristics for single GBs of ZnO have been carried out using bicrystals.[5–7] The model experiments on GBs of ZnO bicrystals[7] showed that the crystallographic anisotropy of the GB properties plays a crucial role in varistor functions. Figure 1 explains nomenclature used in this paper to describe different GBs and IBs. Specifically, $[\mathbf{C}^{-}(000\bar{1})|\mathbf{C}^{-}(000\bar{1})]$ bicrystal junctions exhibit significant barrier effects and upon proper chemical modification even varistorlike breakdown behaviors, while the single junctions in $[\mathbf{C}^{+}(0001)|\mathbf{C}^{+}(0001)]$ configuration exhibit little barrier effects at all conditions. Thereby, it was proposed as a working mechanism that the height of the Schottky barrier at the GB is affected by the presence of an intrinsic electric field that points toward (0001) plane in ZnO due to its inherent polarity.[7,8] The results indicate that although IBs themselves contribute little to the varistor functions, GBs with a specific polarity imposed by the presence of IBs do. Note that the presence of IBs in the individual grains directly affects the crystallographic directions and the polarities of outer GB planes. For example, when the IBs are in a so-called head-to-head configuration as exemplarily shown in Fig. 2(a), the outer GBs of usual convex shaped grains can only have $\mathbf{C}^{-}(000\bar{1})$ planes and nonbasal planes. On the other hand, when the IBs are in a tail-to-tail configuration as shown in Fig. 2(b), the GBs have mostly $\mathbf{C}^{+}(0001)$ basal planes.

To have a better understanding of the effect of the GB polarities on the varistor functions, we prepared $ZnO–Bi_2O_3$ specimens with reagent graded powders, one of which has head-to-head IBs from the addition of Sb[9–11] and the other of which contains tail-to-tail IBs by doping Ti.[10,12] To facilitate the formation of the tail-to-tail IBs, a $Bi_4Ti_3O_{12}$ powder was presynthesized at 750 °C for 2 h using a powder mixture of $40Bi_2O_3–60TiO_2$.[13] The final composition of each specimen was $99.7ZnO–0.12Bi_2O_3–0.18Sb_2O_3$ (SBZ) and $99.6ZnO–0.4Bi_4Ti_3O_{12}$ (TBZ), respectively. In the meantime, $99.8ZnO–0.12Bi_2O_3$ (BZ), which does not have IB inside grains, was also prepared as a reference. All the green compacts were sintered at 1200 °C for 8 h, embedded in the atmospheric powder with the same composition to minimize the evaporation of Bi_2O_3. To obtain homogeneous microstructure, each specimen was sintered at a different heating rate. The optimized process was a standard heating of 5 °C/min for SBZ and BZ, while a rapid heating for TBZ.

Microstructure characterization was performed on a polished and chemically etched surface by scanning electron microscope (SEM, JSM-6360, Japan) as shown in Fig. 2. It was determined by the intercept method[14] that the grain size distribution of each sample was narrow, and the average

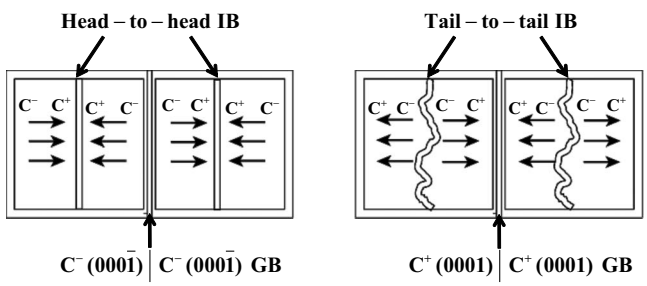

FIG. 1. The nomenclature used to describe different GBs and IBs.

a)Author to whom correspondence should be addressed. Electronic mail: pchan@snu.ac.kr.
b)Presently at the University of Ulsan, Ulsan, Korea.

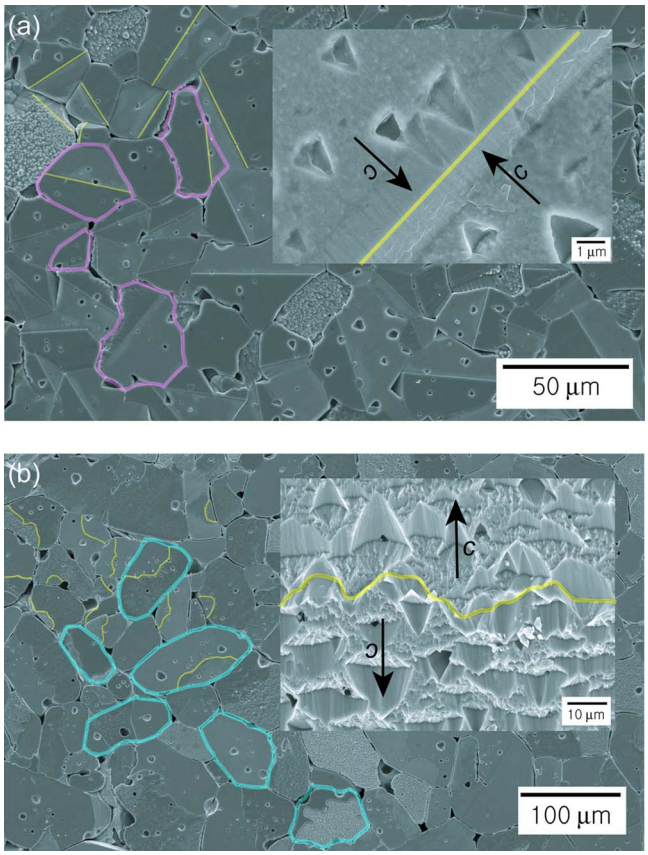

FIG. 2. (Color online) SEM images of ZnO polycrystals containing (a) Sb and (b) Ti. Within the individual grains the IBs indicated by straight lines in (a) and meandering lines in (b) bisect the grains marked by the closed contours. The polarity inversion is clearly distinguished by the etching pattern of the grains (see the insets).

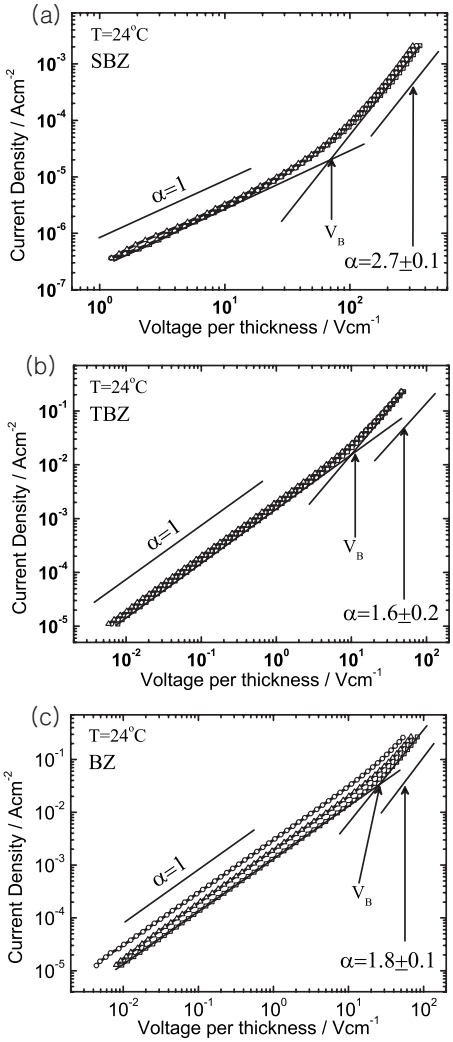

FIG. 3. *I-V* characteristics of (a) SBZ, (b) TBZ, and (c) BZ specimens.

sizes of SBZ, TBZ, and BZ are 40, 100, and 40 μm, respectively. The etch contrast clearly distinguishes the two domains in the individual grains separated by IBs. The polarity of each domain is identified simply by the shape of chemically induced etch pits without recourse to detailed high resolution electron diffraction studies[9,15,16] because the chemical reactivity of ZnO crystals depends significantly on their crystallographic orientation.[16,17] A triangular shape of etch pits in the inset figures clearly shows that only head-to-head IBs are present in SBZ while tail-to-tail ones in TBZ.

Based on our preliminary tests on various electrode materials, Ti/Au films, which is known to form an Ohmic contact with *n*-type ZnO, have been chosen. Relatively large batch-to-batch deviation in the electrical properties of TBZ, which is likely to be due to an inhomogeneous distribution of Ti-rich second phases, was safely overcome by mixing and grinding the powders more thoroughly and repetitively. Thereby, we obtained more or less homogeneous *I-V* responses from all nine specimens out of the same batch for each composition as shown in Fig. 3(a). The measurements were performed at room temperature in air using a source measure unit (236 Keithley, USA) with Ti/Au (80–100/500–600 nm) as an electrode. Figures 3(a)–3(c) show the *I-V* characteristics of SBZ, TBZ, and BZ, respectively. It is evident that all specimens exhibit a varistorlike nonlinear feature to a certain degree. It is interesting to note that there is practically no difference in *I-V* characteristics between TBZ and BZ, while SBZ specimens exhibit a larger resistance in an Ohmic region (by a factor of 10^3) and the nonlinear coefficient $\alpha(d \log I / d \log V)$ of about 1.5–2 times as large as those of the others. The breakdown bias (V_B) indicated in Fig. 3 is determined as the voltage at the onset of the nonlinearity. The "breakdown" bias per grain was estimated to be 0.21 ± 0.03 V for SBZ, 0.10 ± 0.02 V for TBZ, and 0.11 ± 0.02 for BZ, which is fairly consistent with the results from the single junction experiments.[7,18,19]

Considering that electric current follows the path of the lowest resistance, the currently observed *I-V* features of each system strongly indicates that the easy path for the electric current of TBZ and BZ is practically identical and SBZ has its unique path. It should be noted that SBZ and TBZ lack a specific type of GBs, i.e., [$\mathbf{C}^+(0001)$|any plane] and [$\mathbf{C}^-(000\bar{1})$|any plane], respectively, while BZ has all the possible configurations, and that [non-basal|non-basal] GBs should form a continuous network throughout the samples for all three cases. Based on these facts, we can reasonably assume that the major conduction path for all systems is [non-basal|non-basal] GBs. The inferior varistor properties of TBZ and BZ can be attributed to the presence of [$\mathbf{C}^+(0001)$|non-basal] GBs, which could frequently appear along the [non-basal|non-basal] GB networks. Note that [$\mathbf{C}^+(0001)$|non-basal] GBs are known to have practically negligible Schottky barrier height.[7]

Further characterization on the GB barriers was performed by zero-bias impedance analysis using a frequency response analyzer (Solartron 1260, U.K.) together with a dielectric interface (Solartron 1269, U.K.) with ac 10 mV on the samples mounted on a closed cycle refrigerator (Janis, USA) for the temperature range of −75 °C and 220 °C. The bulk resistance at the high frequency intercept was too small to be reliably estimated and thus neglected. The effective capacitance of GB barrier was defined using a relaxation time constant τ from the peak frequency following $C_{gb} \equiv \tau R^{-1}$. The brick layer model enabled the estimation of double Schottky depletion layers (d) to be estimated as 90–110 nm for SBZ, 9–15 nm for TBZ, and 10–28 nm for BZ from the relation $d=D\times C_{bulk}/C_{gb}$ using the dielectric constant of ZnO (~8) and the grain size D determined from the microstructure.[20] From the Schottky barrier model and the assumption that both SBZ and TBZ have similar bulk dopant concentrations, these capacitance values indicate the boundary potential in SBZ ca. three times as high as that in TBZ.

Through a carefully designed polarity engineering of $ZnO-Bi_2O_3$ based varistor ceramics, the crystallographic aspects of the GBs are found to have a significant influence on the electrical properties. Comparison of the *I-V* characteristics and zero-bias ac behavior strongly suggests that aligning the GBs coupled with $\mathbf{C}^{-}(000\bar{1})$ plane by the use of such dopants as Sb enables the performance of ZnO varistor to exhibit superior varistor properties.

This work was supported by the Korea Research Foundation Grant funded by the Korean Government (MOEHRD, Basic Research Promotion Fund) (Grant No. KRF-2008-314-D00174). J.-S. Lee acknowledges the support by the Korea Research Foundation Grant funded by the Korean Government (MOEHRD) (Grant No. KRF-2007-331-D00195).

[1]T. K. Gupta, J. Am. Ceram. Soc. **73**, 1817 (1990).
[2]F. Greuter and G. Blatter, Semicond. Sci. Technol. **5**, 111 (1990).
[3]B. A. Haskell, S. J. Souri, and M. A. Helfand, J. Am. Ceram. Soc. **82**, 2106 (1999).
[4]M. Tao, B. Ai, O. Dorlanne, and A. Loubiere, J. Appl. Phys. **61**, 1562 (1987).
[5]Y. Sato, T. Mizoguchi, F. Oba, M. Yodogawa, T. Yamamoto, and Y. Ikuhara, Appl. Phys. Lett. **84**, 5311 (2004).
[6]Y. Sato, T. Yamamoto, and Y. Ikuhara, J. Am. Ceram. Soc. **90**, 337 (2007).
[7]J.-S. Lee and J. Maier, J. Mater. Res. **20**, 2101 (2005).
[8]P. M. Verghese and D. R. Clarke, J. Appl. Phys. **87**, 4430 (2000).
[9]A. Recnik, N. Daneu, T. Walther, and W. Mader, J. Am. Ceram. Soc. **84**, 2657 (2001).
[10]D. Makovec, D. Kolar, and M. Trontelj, Mater. Res. Bull. **28**, 803 (1993).
[11]N. Daneu, A. Rečnik, S. Bernik, and D. Kolar, J. Am. Ceram. Soc. **83**, 3165 (2000).
[12]D. F. K. Hennings, R. Hartung, and P. J. L. Reijnen, J. Am. Ceram. Soc. **73**, 645 (1990).
[13]J.-W. Lee, Master's thesis, Seoul National University, 2004.
[14]J.-H. Han and D.-Y. Kim, Acta Metall. Mater. **43**, 3185 (1995).
[15]J.-C. Kim and E. Goo, J. Am. Ceram. Soc. **73**, 877 (1990).
[16]W. Jo, S.-J. Kim, and D.-Y. Kim, Acta Mater. **53**, 4185 (2005).
[17]A. N. Mariano and R. E. Hanneman, J. Appl. Phys. **34**, 384 (1963).
[18]R. Einzinger, Appl. Surf. Sci. **3**, 390 (1979).
[19]E. Olsson and G. L. Dunlop, J. Appl. Phys. **66**, 3666 (1989).
[20]J.-S. Lee and D.-Y. Kim, J. Mater. Res. **16**, 2739 (2001).